Progress In Electromagnetics Research, Vol. 105, 157–170, 2010

APPLICATION OF ICA TECHNIQUE TO PCA BASED RADAR TARGET RECOGNITION

C.-W. Huang and K.-C. Lee

Department of Systems and Naval Mechatronic Engineering
National Cheng-Kung University
Tainan 701, Taiwan

Abstract—In this paper, the ICA (independent component analysis) technique is applied to PCA (principal component analysis) based radar target recognition. The goal is to identify the similarity between the unknown and known targets. The RCS (radar cross section) signals are collected and then processed to serve as the features for target recognition. Initially, the RCS data from targets are collected by angular-diversity technique, i.e., are observed in directions of different elevation and azimuth angles. These RCS data are first processed by the PCA technique to reduce noise, and then further processed by the ICA technique for reliable discrimination. Finally, the identification of targets will be performed by comparing features in the ICA space. The noise effects are also taken into consideration in this study. Simulation results show that the recognition scheme with ICA processing has better ability to discriminate features and to tolerate noises than those without ICA processing. The ICA technique is inherently an approach of high-order statistics and can extract much important information about radar target recognition. This property will make the proposed recognition scheme accurate and reliable. This study will be helpful to many applications of radar target recognition.

1. INTRODUCTION

The radar target recognition means to identify unknown targets from observed signals. It plays an important role in the radar engineering. This study focuses on the radar recognition of ships. Traditionally, the SAR (synthetic aperture radar) or ISAR (inverse synthetic aperture radar) images are usually utilized to recognize the ship targets,

Corresponding author: K.-C. Lee (kclee@mail.ncku.edu.tw).

e.g., [1, 2]. However, it is usually expensive or even difficult to obtain such SAR or ISAR images. Compared with SAR or ISAR images, the RCS (radar cross section) [3] data are easy to obtain and then become good candidates for radar target recognition of ships [4]. In [4], we have successfully utilized angular-diversity RCS data in PCA (principal component analysis) [5] space as features to identify radar targets. The PCA based radar target recognition [4] means the original signals are projected into a low-dimensional eigenspace and identification of targets is performed in the eigenspace. The major drawback of PCA based radar target recognition [4] is that the PCA technique can treat dependencies of features only to the second-order statistics and may lose some useful information about target identification. This then motivates us to develop a new scheme of radar target recognition based on high-order statistics. Since the ICA (independent component analysis) [6] technique can treat dependencies of features to high-order statistics, it then becomes a good candidate in our new scheme of radar target recognition.

The ICA is a statistical and computational technique for revealing hidden factors that underlies sets of random variables, measurements, or signals. The data analyzed by ICA could originate from many different kinds of application fields, such as digital images, document databases, psychometric measurements, etc. In this paper, the ICA [6] technique is applied to PCA [5] based radar target recognition [4]. Without loss of generality, models of ships are considered as the targets for recognition. It should be noted that our recognition scheme has no limitation on types of targets. The main reason why we focus on models of ships is that the results of this paper can be compared with our past studies [4]. Our recognition scheme is divided into four (including three off-line and one on-line) steps. Initially, the RCS data from ships are collected by angular-diversity technique, i.e., are observed in directions of different elevation and azimuth angles. These RCS data are first processed by the PCA technique to reduce noise, and then further processed by the ICA technique for reliable discrimination. Finally, the identification of targets will be performed by comparing features in the ICA space. The noise effects are also taken into consideration in this study. Simulation results show that the recognition scheme with ICA processing has better ability to discriminate features and to tolerate noises than those without ICA processing. This is due to the high-order statistical properties of ICA technique.

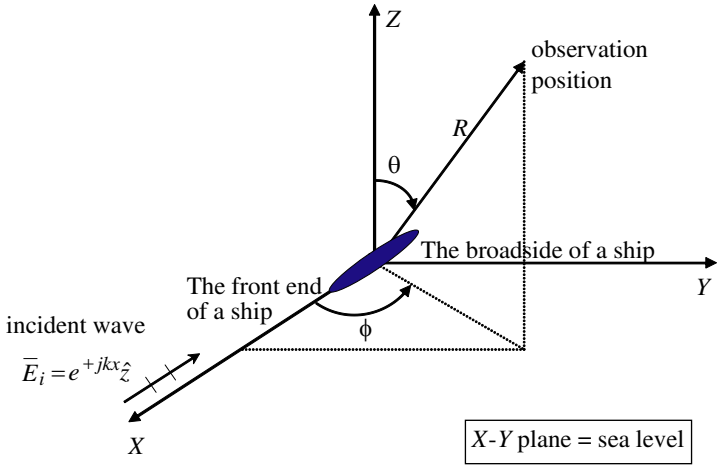

Figure 1. Schematic diagram of a ship illuminated by an incident plane wave.

2. FORMULATIONS

Without loss of generality, the targets for the proposed radar recognition algorithm are chosen as ships. It should be noted that this study has no limitation in types of targets. Consider a ship on the sea level (X-Y plane) located at the origin of coordinate, as shown in Figure 1. The front end of ship is in the $+\hat{x}$ direction and the broadside of ship is in the $+\hat{y}$ direction. The spherical coordinate system is defined as (ρ, θ, ϕ) where ρ is the distance from observation position to origin, θ is the elevation angle and ϕ is the azimuth angle. The ship is illuminated by a plane wave $\overline{E}_i = e^{+jkx}\hat{z}$ (i.e., propagating toward the $-\hat{x}$ direction) where k is the wavenumber. The bistatic RCS in the direction of (θ, ϕ) is defined as [3]

$$RCS = \lim_{\rho \to \infty} 4\pi\rho^2 \frac{\left|\overline{E}_s(\theta, \phi)\right|^2}{\left|\overline{E}_i\right|^2}. \tag{1}$$

where $\overline{E}_s(\theta, \phi)$ is the scattered electric field.

In this study, the RCS data in different directions are collected for target recognition. Both PCA and ICA techniques are utilized in our target recognition scheme. Our target recognition scheme includes off-line and on-line procedures, as described in the following.

Step-1: constructing RCS databases (off-line)

Initially, RCS databases of known ships are constructed. Assume we have C types of known ships. The bistatic RCS data for each type of known ship (e.g., type $\sharp c$, $c = 1, \ldots, C$) are collected in directions of N_e different elevation angles (θ) and N_a different azimuth angles (ϕ) to constitute an $N_a \times N_e$ RCS matrix (for type $\sharp c$, denoted as $\overline{\overline{X}}_c$). Obviously, we have C measured matrices totally since there are C types of known ships. These C measured matrices are combined together to constitute a large RCS matrix as

$$\overline{\overline{R}}_{N_a \times (N_e C)} = \left[\overline{\overline{X}}_1 \overline{\overline{X}}_2 \ldots \overline{\overline{X}}_C \right]_{N_a \times (N_e C)} . \tag{2}$$

Step-2: PCA processing (off-line)

The collected RCS data in Step-1 are first processed by the following PCA technique for reducing the noise. Assume the mean vector for all the $(N_e C)$ column vectors of matrix $\overline{\overline{R}}$ in (2) is $\overline{\mu}_r$ (dimension $N_a \times 1$). The centered matrix for $\overline{\overline{R}}$ is then given as

$$\overline{\overline{Z}}_{N_a \times (N_e C)} = \overline{\overline{R}}_{N_a \times (N_e C)} - [\overline{\mu}_r, \overline{\mu}_r, \ldots, \overline{\mu}_r]_{N_a \times (N_e C)} . \tag{3}$$

Consider the covariance matrix $(\overline{\overline{Z}} \cdot \overline{\overline{Z}}^T)_{N_a \times N_a}$, where "$T$" denotes the transpose. In general, the N_a is large and it is inefficient to calculate eigenvalues of the covariance matrix. Since only the principal eigenvalues and eigenvectors are required in the PCA processing, the Karhunen-Loève's low-rank approximation [5] may be utilized to obtain the required eigenvalues and eigenvectors. In other words, eigenvalues and eigenvectors of the low-rank matrix $(\overline{\overline{Z}}^T \cdot \overline{\overline{Z}})_{(N_e C) \times (N_e C)}$ are considered instead. Note that we have $N_e C \ll N_a$ in general. The eigenvalues are calculated and ranked decreasingly as $\lambda_1 \geq \lambda_2 \geq \ldots$. Their corresponding eigenvectors are denoted as $\overline{\phi}_1, \overline{\phi}_2, \ldots$. In the PCA processing, only the top P ($P < N_e C < N_a$) eigenvalues $\lambda_1, \lambda_2, \ldots, \lambda_P$ are reserved as the "principal components" and the other eigenvalues are discarded. The principal eigenvectors $\overline{\phi}_1, \overline{\phi}_2, \ldots, \overline{\phi}_P$ will constitute a matrix as

$$\overline{\overline{A}}_{(N_e C) \times P} = \left[\overline{\phi}_1, \overline{\phi}_2, \ldots, \overline{\phi}_P \right] . \tag{4}$$

The PCA projection matrix is then defined as

$$\overline{\overline{B}}_{N_a \times (N_e C)} = \overline{\overline{Z}} \cdot \overline{\overline{A}} \cdot \overline{\overline{A}}^T + [\overline{\mu}_r, \overline{\mu}_r, \ldots, \overline{\mu}_r]_{N_a \times (N_e C)} . \tag{5}$$

In general, the PCA projection matrix $\overline{\overline{B}}_{N_a \times (N_e C)}$ in (5) is much cleaner, i.e., with less noise, than the original measurement $\overline{\overline{Z}}$.

Step-3: ICA processing (off-line)

In this step, The PCA projection matrix in (5) of Step-2 are further processed by the ICA technique. For convenience, the feature matrix $\overline{\overline{B}}$ in (5) is transposed and then horizontally divided into C equal sub-matrices, i.e.,

$$\overline{\overline{B}}^{T} = \begin{bmatrix} \left(\overline{\overline{Y}}_1\right)_{N_e \times N_a} \\ \left(\overline{\overline{Y}}_2\right)_{N_e \times N_a} \\ \vdots \\ \left(\overline{\overline{Y}}_C\right)_{N_e \times N_a} \end{bmatrix}_{(N_e C) \times N_a} . \tag{6}$$

Note that the sub-matrix $\overline{\overline{Y}}_c$ $(c = 1, 2, \ldots, C)$ represents the contribution of PCA projection from the known ship of type $\sharp c$. Based on the concept of ICA, each sub-matrix $\overline{\overline{Y}}_c$ $(c = 1, 2, \ldots, C)$ can be viewed as the linear combination of several independent sources or

$$\left(\overline{\overline{Y}}_c\right)_{N_e \times N_a} = \left(\overline{\overline{A}}_c\right)_{N_e \times N_e} \cdot \left(\overline{\overline{S}}_c\right)_{N_e \times N_a} . \tag{7}$$

In (7), the matrix $(\overline{\overline{S}}_c)_{N_e \times N_a}$ contains N_e row vectors representing independent sources, and the matrix $(\overline{\overline{A}}_c)_{N_e \times N_e}$ contains coefficients of linear combination. From (7), we have

$$\left(\overline{\overline{S}}_c\right)_{N_e \times N_a} = \left(\overline{\overline{W}}_c\right)_{N_e \times N_e} \cdot \left(\overline{\overline{Y}}_c\right)_{N_e \times N_a} . \tag{8}$$

where $\overline{\overline{W}}_c = (\overline{\overline{A}}_c)^{-1}$ is the demixing matrix. In this study, the values of $\overline{\overline{W}}_c$ are computed from the FastICA iteration algorithm [6]. The detailed procedures of FastICA algorithm are given in [6].

The next step is to whiten the matrix $\overline{\overline{Y}}_c$. Assume $\mu_{c,i}$ denotes the mean for elements in the i-th row of the matrix $\overline{\overline{Y}}_c$. The centered matrix of $\overline{\overline{Y}}_c$ is given as

$$\left(\overline{\overline{\Omega}}_c\right)_{N_e \times N_a} = \left(\overline{\overline{Y}}_c\right)_{N_e \times N_a} - \begin{bmatrix} \mu_{c,1} & \mu_{c,1} & \cdots & \mu_{c,1} \\ \mu_{c,2} & \mu_{c,2} & \cdots & \mu_{c,2} \\ \vdots & \vdots & \vdots & \vdots \\ \mu_{c,N_e} & \mu_{c,N_e} & \cdots & \mu_{c,N_e} \end{bmatrix}_{N_e \times N_a} . \tag{9}$$

The covariance matrix is defined as

$$\left(\overline{\overline{C}}_{\Omega_c}\right)_{N_e \times N_e} = \overline{\overline{\Omega}}_c \cdot \overline{\overline{\Omega}}_c^{\,T} . \tag{10}$$

The whitening of $\overline{\overline{Y}}_c$ is then given as

$$\left(\overline{\overline{H}}_c\right)_{N_e\times N_a} = \left(\overline{\overline{D}}_c^{\,-\frac{1}{2}}\right)_{N_e\times N_e} \cdot \left(\overline{\overline{E}}_c^{\,T}\right)_{N_e\times N_e} \cdot \left(\overline{\overline{\Omega}}_c\right)_{N_e\times N_a}. \quad (11)$$

In (11), the matrix $\overline{\overline{D}}_c$ is a diagonal matrix with elements given from eigenvalues of matrix $\overline{\overline{C}}_{\Omega_c}$, and the matrix $\overline{\overline{E}}_c$ has column vectors given from eigenvectors of matrix $\overline{\overline{C}}_{\Omega_c}$. Therefore, new ICA projection matrices can be defined as $(\overline{\overline{W}}_c \cdot \overline{\overline{H}}_c)_{N_e\times N_a}$ $(c = 1, 2, \ldots, C)$. These new ICA projection matrices will be utilized as the final features in identifying the targets, as shown in the following step.

Step-4: Testing (on-line)

In this step, the on-line testing, i.e., recognition for unknown targets is given. As an unknown ship is detected on the sea surface, its bistatic RCS data are first collected in directions of N_e different elevation angles (θ) and N_a different azimuth angles (ϕ) to constitute an $N_a \times N_e$ RCS matrix $\overline{\overline{X}}$. Initially, it is processed by the PCA technique. The procedures of PCA processing are similar to those given in Step-2, except that the $N_a \times (N_eC)$ matrix $\overline{\overline{R}}$ is replaced by the $N_a \times N_e$ matrix $\overline{\overline{X}}$. As a result, the dimension of matrix $\overline{\overline{B}}$ in (5) becomes $N_a \times N_e$. In other words, the dimension of matrix $\overline{\overline{B}}^T$ in (6) becomes $N_e \times N_a$. Therefore, the right side of (6) is composed of only one sub-matrix and this sub-matrix is denoted as $\overline{\overline{Y}}$. The matrix $\overline{\overline{Y}}$ is whitened into a new matrix and the result is denoted as $\overline{\overline{H}}$. The whitening procedures are similar to those given in (9)–(11) except that the matrix $\overline{\overline{Y}}_c$ is replaced by $\overline{\overline{Y}}$.

The difference matrix (in ICA space) between the unknown target and the known ship of type $\sharp c$ $(c = 1, 2, \ldots, C)$ is defined as

$$\overline{\overline{D}}_c = \overline{\overline{W}}_c \cdot \left(\overline{\overline{H}} - \overline{\overline{H}}_c\right), \; c = 1, 2, \ldots, C. \quad (12)$$

Note that the matrix $\overline{\overline{D}}_c$ in (12) contains the difference information about features in ICA space under various observing directions. For example, the magnitude for the i-th row vector of matrix $\overline{\overline{D}}_c$ (denoted as $m_{c,i}$) represents the difference (in ICA space) with respect to the known ship of type $\sharp c$ as the unknown target is observed in direction of the i-th elevation angle. In such a case, the "similarity" is defined as

$$similarity = 1 - \frac{m_{c,i}}{\sum_{c=1}^{C} m_{c,i}}, \; i = 1, 2, \ldots, N_e. \quad (13)$$

The above definition means the strong resemblance has a large value of "*similarity*", and vice versa.

3. NUMERICAL SIMULATION RESULTS

In this section, numerical examples are given to verify the above formulations. To simplify the computation, simple ship models are considered instead of practical ships. The RCS data are calculated by using the commercial software Ansoft HFSS which has been proved to be accurate by many researchers in electromagnetic waves. Assume there are three types of known ships (i.e., $C = 3$) including type ♯1 (to model the container vessel), type ♯2 (to model the naval ship) and type ♯3 (to model the fishing boat). The geometrical models for these three types of known ships are shown in Figure 2. The ship length l is chosen as $kl = 9.4$ for the ship of type ♯1, $kl = 6.3$ for the ship of type ♯2, and $kl = 3.1$ for the ship of type ♯3, where k is the wavenumber. All ships are on a rough sea level (X-Y plane) and the characteristic for surface roughness of sea level is assumed to be sinusoidal as

$$z(x, y) = \frac{4}{75} l \cdot \sin\left(\frac{15}{4}\pi x\right) \sin\left(\frac{15}{4}\pi y\right) + \frac{8}{75} l. \tag{14}$$

The sea water has dielectric constant $\varepsilon_r = 81$ and conductivity $\sigma = 4\,\mathrm{S/m}$. There are three examples in the following to verify the proposed target recognition scheme.

In the first example, the unknown target is assumed to be the ship of type ♯1. As the arrangement in Figure 1, the bistatic RCS from each

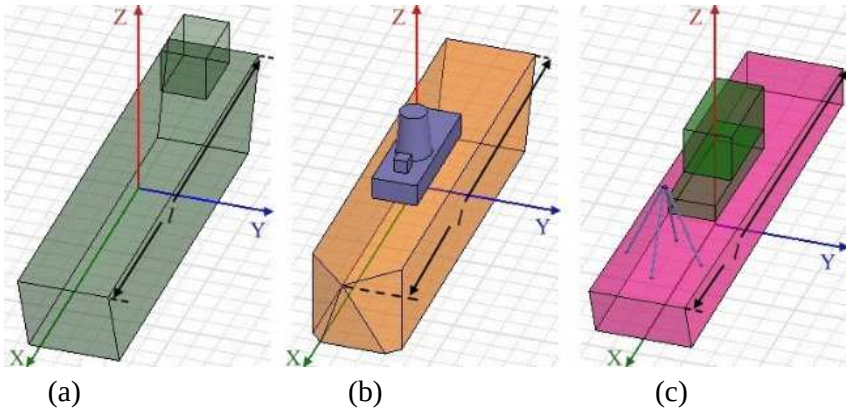

Figure 2. The geometrical models for the three types of known ships: (a) type ♯1, (b) type ♯2 and (c) type ♯3.

type of known ship in directions of a fixed elevation angle θ and 181 (i.e., $N_a = 181$) azimuth angles of $\phi = 0°, 1°, \ldots, 180°$ are collected to constitute a column vector. To make our recognition believable, the sampling elevation angles for training (i.e., off-line) and testing (i.e., on-line) are different. In our simulation, elevation angles are chosen to be $\theta = 61°, 63°, \ldots, 89°$ for training and $\theta = 62°, 64°, \ldots, 90°$ for testing, respectively. In other words, the N_e in Section 2 is equal to 15. In Step-2 of Section 2, the number of principal components is chosen to be $p = 2$. The selection of p is according to research experiences in this field. In general, the higher eigenvalues represent the signal subspace, whereas the lower eigenvalues represent the noise subspace [6]. The radar recognition algorithm is trained using Step-1 to Step-3 (off-line stages) in Section 2. After the algorithm is well trained, it can identify the unknown target of ship by using the Step-4 (on-line stage) in Section 2. Following the recognition procedures of Section 2, the similarity between the unknown target and the three types of known ships at all the 15 testing elevation angles of θ is shown in Figure 3. According to (13), the largest similarity, i.e., the highest line of Figure 3, means this type of known ship (type ♯1) has the most resemblance to the unknown target. In Figure 3(a), only the PCA technique [4] is utilized. The average similarity of the 15 testing elevation angles is 0.897 to type ♯1, 0.811 to type ♯2 and 0.285 to

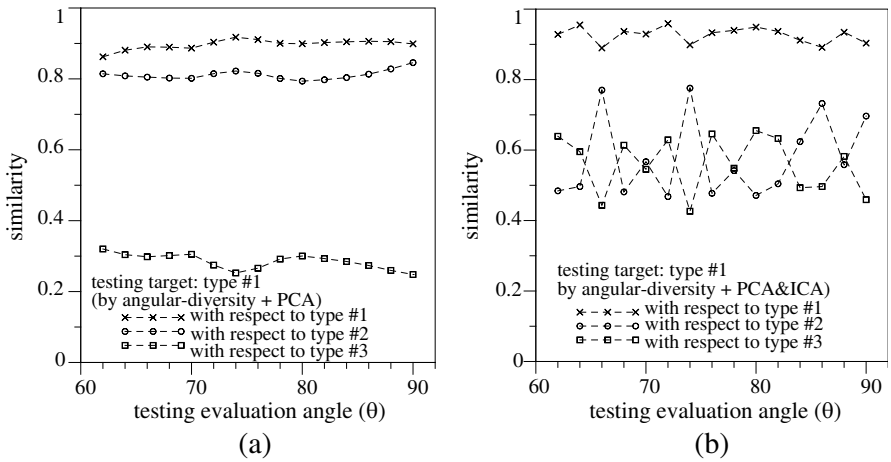

Figure 3. The similarity between the unknown target (i.e., the ship of type ♯1 in the first example) and the three types of known ships at all the 15 testing elevation angles of θ: (a) by PCA technique only, (b) by proposed PCA & ICA techniques.

type ♯3. In Figure 3(b), the "PCA & ICA" techniques in Section 2 of this paper are utilized. The average similarity of the 15 testing elevation angles is 0.926 to type ♯1, 0.577 to type ♯2 and 0.560 to type ♯3. Both Figures 3(a) and 3(b) show that the known ship of type ♯1 has the highest similarity, i.e., resembles the unknown target most. This result is very reasonable because the testing target is just the ship of type ♯1. The recognition results are correct at all the 15 testing evaluation angles and then the successful recognition rate is $15/15 = 100\%$. In our simulation, the discrimination can be defined as the difference between the best and the next-best similarity. Under this definition, the average discrimination is 0.086 $(= 0.897 - 0.811)$ for Figure 3(a), and is 0.349 $(= 0.926 - 0.577)$ for Figure 3(b). This means that Figure 3(b) by "PCA & ICA" has better discriminating ability than Figure 3(a) by "PCA" only. In other words, the add of ICA technique to the PCA based recognition will improve the discriminating ability.

In the second example, the unknown target is assumed to be the ship of type ♯2. The recognition procedures are the same as those given in the first example. Figure 4 shows the similarity between the unknown target and the three types of known ships at all the 15 testing elevation angles of θ. In Figure 4(a), only the PCA technique [4] is utilized. The average similarity of the 15 testing elevation angles is

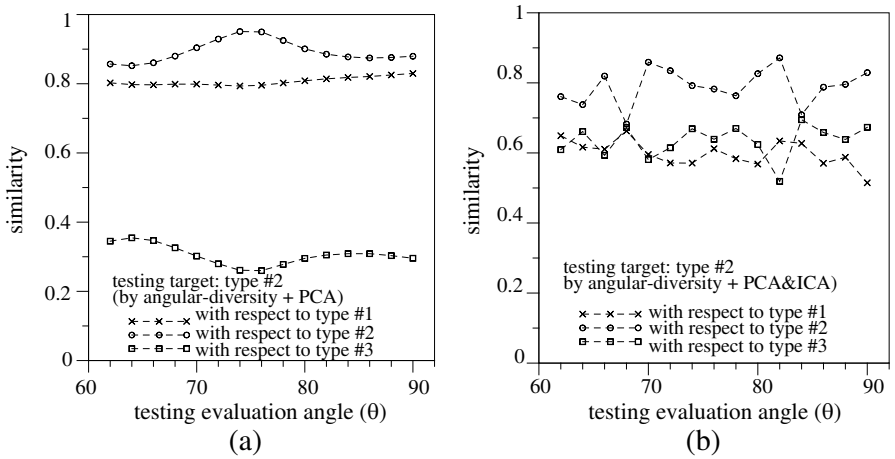

Figure 4. The similarity between the unknown target (i.e., the ship of type ♯2 in the second example) and the three types of known ships at all the 15 testing elevation angles of θ: (a) by PCA technique only, (b) by proposed PCA & ICA techniques.

0.807 to type ♯1, 0.893 to type ♯2 and 0.305 to type ♯3. In Figure 4(b), the "PCA & ICA" techniques in Section 2 of this paper are utilized. The average similarity of the 15 testing elevation angles is 0.598 to type ♯1, 0.790 to type ♯2 and 0.634 to type ♯3. Both Figure 4(a) and Figure 4(b) show that the known ship of type ♯2 has the highest similarity, i.e., resembles the unknown target most. This result is very reasonable because the testing target is just the ship of type ♯2. The recognition results are correct at all the 15 testing evaluation angles and then the successful recognition rate is $15/15 = 100\%$. The average discrimination is 0.086 ($= 0.893 - 0.807$) for Figure 4(a), and is 0.156 ($= 0.790 - 0.634$) for Figure 4(b). This means that Figure 4(b) by "PCA & ICA" has better discriminating ability than Figure 4(a) by "PCA" only. In other words, the add of ICA technique to the PCA based recognition will improve the discriminating ability.

In the third example, the unknown target is assumed to be the ship of type ♯3. The recognition procedures are the same as those given in the previous examples. Figure 5 shows the similarity between the unknown target and the three types of known ships at all the 15 testing elevation angles of θ. In Figure 5(a), only the PCA technique [4] is utilized. The average similarity of the 15 testing elevation angles is 0.532 to type ♯1, 0.541 to type ♯2 and 0.928 to type ♯3. In Figure 5(b), the "PCA & ICA" techniques in Section 2 of this paper

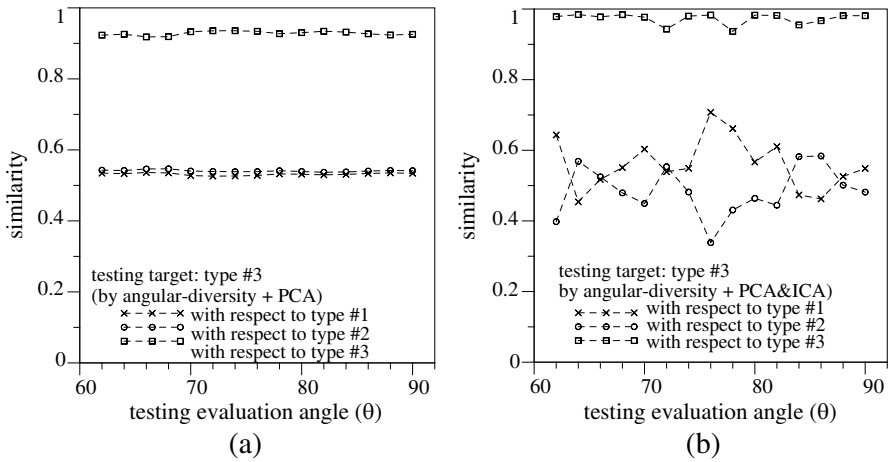

Figure 5. The similarity between the unknown target (i.e., the ship of type ♯3 in the third example) and the three types of known ships at all the 15 testing elevation angles of θ: (a) by PCA technique only, (b) by proposed PCA & ICA techniques.

are utilized. The average similarity of the 15 testing elevation angles is 0.561 to type ♯1, 0.485 to type ♯2 and 0.973 to type ♯3. Both Figures 5(a) and 5(b) show that the known ship of type ♯3 has the highest similarity, i.e., resembles the unknown target most. This result is very reasonable because the testing target is just the ship of type ♯3. The recognition results are correct at all the 15 testing evaluation angles and then the successful recognition rate is $15/15 = 100\%$. The average discrimination is 0.387 ($= 0.928 - 0.541$) for Figure 5(a), and is 0.412 ($=0.973 - 0.561$) for Figure 5(b). This means that Figure 5(b) by "PCA & ICA" has better discriminating ability than Figure 5(a) by "PCA" only. In other words, the add of ICA technique to the PCA based recognition will improve the discriminating ability.

Practically, the measured RCS includes random noise. To investigate the effects of noise, each calculated RCS is added by an independent random noise. The noise is assumed to be with Gaussian distribution and zero mean. For convenience, the standard derivation of noise is normalized with respect to the root mean square of calculated RCS. In our simulation, the noise level, i.e., the normalized standard derivation of noise, is assumed to be 10^{-4}, 10^{-3}, 10^{-2}, 10^{-1}, 2×10^{-1} and 4×10^{-1}, respectively. The number of trials for each Gaussian distribution is chosen as 10. Figure 6 shows the average

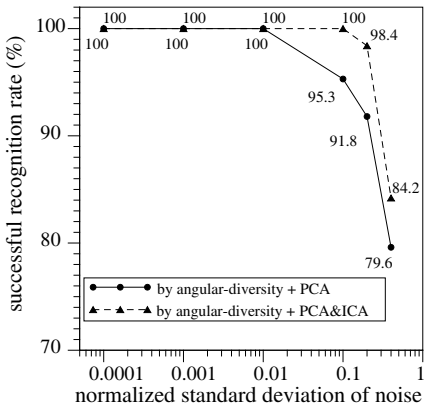

Figure 6. The average successful recognition rate with respect to different levels (i.e., normalized standard derivation) of noise by "PCA" technique only, and by proposed "PCA & ICA" techniques.

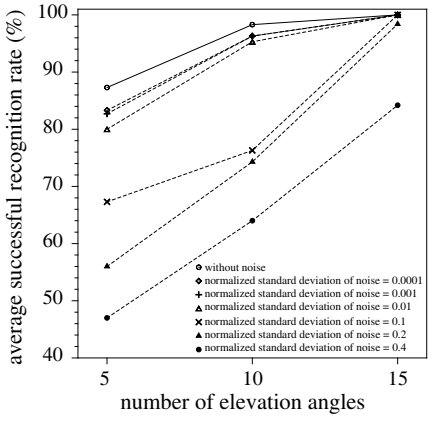

Figure 7. The average successful recognition rate with respect to different number of elevation angles in off-line stages.

successful recognition rate with respect to different levels of noise by "PCA" technique only, and by proposed "PCA & ICA" techniques. From Figure 6, it shows that the successful recognition rates under the above noise levels are 100%, 100%, 100%, 95.3%, 91.8% and 79.6%, by "PCA" technique only. Figure 6 also shows that the successful recognition rates under the above noise levels are increased to 100%, 100%, 100%, 100%, 98.4% and 84.2%, by proposed "PCA & ICA" techniques. In other words, the successful recognition rate in noisy environments will be greatly improved, as the ICA technique is added to the PCA based recognition scheme. With the use of ICA, the proposed recognition scheme can still maintain accurate recognition rate of 84.2%, even though the noise level is increased to 4×10^{-1}. This implies that our recognition scheme can tolerate noises and still maintains accurate recognition rate.

Figure 7 shows the average successful recognition rate with respect to different number of elevation angles in off-line stages. In low-niose (e.g., normalized standard deviation of noise ≤ 0.01) environments, the successful recognition rate is only slightly improved as the number of elevation angles increases. In high-niose (e.g., normalized standard deviation of noise ≥ 0.1) environments, the successful recognition rate is greatly improved as the number of elevation angles increases.

4. CONCLUSION

In this paper, the high-order statistical approach of ICA is successfully applied to PCA based radar target recognition. Simulation results show that the recognition scheme with ICA processing has better ability to discriminate features and to tolerate noises than those without ICA processing. Although the PCA processing can reduce the noise, it treat dependencies of features only to the second-order statistics. The ICA technique is inherently a high-order statistical approach and can extract much important information about radar target recognition. Basically, the ICA can be viewed as an extension of PCA and factor analyses [6]. With the use of ICA, the discriminating ability to identify targets is greatly improved. Noted that this paper is a primary study of applying ICA technique to PCA based radar target recognition. Therefore, many ideal assumptions are made for simplicity. In this paper, the RCS data of a single frequency are collected in many directions. Although the number of observation directions for RCS is high in this paper, this can be improved in the future by frequency-diversity collection of RCS, i.e., RCS of different frequencies are collected in each observation angle. Although this study chooses only simple models of ships as targets of recognition, one can

add different types of random components to RCS for modeling RCS of complex targets. This study can be applied to many other applications in radar target recognition [7–19].

REFERENCES

1. Hajduch, G., J. M. Le Caillec, and R. Garello, "Airborne high-resolution ISAR imaging of ship targets at sea," *IEEE Transactions on Aerospace and Electronic Systems*, Vol. 40, No. 1, 378–384, 2004.
2. Tello, M., C. Lopez-Martinez, and J. J. Mallorqui, "A novel algorithm for ship detection in SAR imagery based on the wavelet transform," *IEEE Geoscience and Remote Sensing Letters*, Vol. 2, No. 2, 201–205, 2005.
3. Ruck, G. T., D. E. Barrick, W. D. Stuart, and C. K. Krichbaum, *Radar Cross Section Handbook*, Vol. 1, Plenum, New York, 1970.
4. Lee, K. C., J. S. Ou, and C. W. Huang, "Angular-diversity radar recognition of ships by transformation based approaches — Including noise effects," *Progress In Electromagnetic Research*, Vol. 72, 145–158, 2007.
5. Moon, T. K. and W. C. Stirling, *Mathematical Methods and Algorithms for Signal Processing*, Prentice Hall, 2000.
6. Hyvärinen, A., J. Karhunen, and E. Oja, *Independent Component Analysis*, John Wiley, 2001.
7. Wang, C. J., B. Y. Wen, Z. G. Ma, W. D. Yan, and X. J. Huang, "Measurement of river surface currents with UHF FMCW radarsystems," *Journal of Electromagnetic Waves and Applications*, Vol. 21, No. 3, 375–386, 2007.
8. Abdelaziz, A. A., "Improving the performance of an antenna array by using radar absorbing cover," *Progress In Electromagnetics Research Letters,* Vol. 1, 129–138, 2008.
9. Razevig, V. V., S. I. Ivashov, A. P. Sheyko, I. A. Vasilyev, and A. V. Zhuravlev, "An example of holographic radar using at restoration works of historical building," *Progress In Electromagnetics Research Letters,* Vol. 1, 173–179, 2008.
10. Hebeish, A. A., M. A. Elgamel, R. A. Abdelhady, and A. A. Abdelaziz, "Factors affecting the performance of the radar absorbant textile materials of different types and structus," *Progress In Electromagnetics Research B,* Vol. 3, 219–226, 2008.
11. Turhan-Sayan, G., "Real time electromagnetic target classification using a novel feature extraction technique with PCA-based

fusion," *IEEE Trans. Antennas and Propagation*, Vol. 53, No. 2, 766–776, 2005.

12. Kim, K. T., D. K. Seo, and H. T. Kim, "Efficient radar target recognition using the MUSIC algorithm and invariant features," *IEEE Trans. Antennas and Propagation*, Vol. 50, No. 3, 325–337, 2002.
13. Secmen, M. and G. Turhan-Sayan, "Radar target classification method with reduced aspect dependency and improved noise performance using multiple signal classification algorithm," *IET Radar, Sonar and Navigation*, Vol. 3, No. 6, 583–595, 2009.
14. Wu, M., B. Y. Wen, and H. Zhou, "Ionosheric clutter suppression in HF wave radar," *Journal of Electromagnetic Waves and Applications*, Vol. 23, No. 10, 1265–1272, 2009.
15. Soldovieri, F. and N. Romano, "The mutual interaction between the reconfigurable transmitting and receiving antennas in ground penetrating radar surveys," *Journal of Electromagnetic Waves and Applications*, Vol. 23, No. 14/15, 1919–1928, 2009.
16. Yang, M. H., J. Xu, and X. W. Sun, "Velocity error analysis of a K-band dual mode traffic radar," *Progress In Electromagnetics Research B*, Vol. 10, 105–116, 2008.
17. Yan, S., S. He, Z. P. Nie, and J. Hu, "Simulating wide band radar response from PEC targets using phase extracted basis functions," *Progress In Electromagnetics Research B*, Vol. 13, 409–431, 2009.
18. Wu, T., X. Tang, and F. Xiao, "Reserch on the coherent phase noise of millimeter-wave doppler radar," *Progress In Electromagnetics Research Letters*, Vol. 5, 23–34, 2008.
19. Kandar, D., C. K. Sarkar, and R. N. Bera, "Simulation of spread spectrum radar using rake at the receiver end," *Progress In Electromagnetics Research Letters*, Vol. 7, 35–45, 2009.